A Transcriptome Profile Reveals The Regulatory Mechanism of *Verticillium Dahliae* Against *Bacillus*

Wenhui Tian
University of Shihezi
Zhenrui Cheng
University of Shihezi
Junxia Wang
University of Shihezi
Fengfeng Cheng
University of Shihezi
Luping Li
University of Shihezi
Chunxiao Huo
University of Shihezi
Wenxuan Li
University of Shihezi
Shouyan Han
University of Shihezi
Xinyong Guo
University of Shihezi
Aiying Wang (way-sh@126.com)
University of Shihezi

Research Article

Keywords: Verticillium dahliae, Biocontrol, Transcriptome, Resistance mechanism, TOR pathways, Mitophagy, ROS, Cell wall synthesis

Posted Date: August 17th, 2021

DOI: https://doi.org/10.21203/rs.3.rs-779813/v1

Abstract

Background: *Verticillium dahliae*, the causal agent of *Verticillium* wilt, is notoriously invasive in many crops and has been involved in numerous epidemics worldwide. *Bacillus* species, as representatives of biocontrol bacteria, produce a variety of lipopeptides (LPs), which are useful as biofungicides to many pathogenic fungi, including *Verticillium dahliae*. This study will explore the mechanism of resistance of *V. dahliae* to *Bacillus* and biocontrol bacteria.

Results: By using *in vitro* confrontation bioassays, we found that under the stress induced by *Bacillus*, the spore vitality of *V. dahliae* with larger colonies was higher, and more abundant microsclerotia were formed. Then, according to the RNA-Seq analysis, the target of rapamycin (TOR) and mitophagy pathways were enriched among the significantly upregulated 542 genes observed in two co-culture groups with different colony sizes. In addition, in the group of *V. dahliae* with large colonies, the pathways related to cell wall synthesis, microsclerotia formation and the clearance of reactive oxygen species were regulated, and the expression of genes was up-regulated.

Conclusion: This study found that the larger colonies of *V. dahliae* were more resistant to the antagonistic actions of *Bacillus* and the likelihood of the formation of homeostasis. Therefore, the prevention of *Verticillium* wilt by *Bacillus* is more effective than the treatment of an active fungal infection. These transcriptomic insights provide direction for the use of fungicides in the prevention and treatment of diseases such as *Verticillium* wilt.

Background

Verticillium dahliae (Ascomycota, Plectosphaeroliacea) is a soil fungus that causes a wilt disease and early senescence in plants. Its hosts include numerous plant species, including important crops, such as cotton and pepper. In addition, new hosts are continually being identified [1, 2]. *V. dahliae* is difficult to control, since it can survive for decades in the soil without a host plant by forming microsclerotia. Microsclerotia are formed from the fungal hyphae and are found not only in the tissue of affected plants but also in and on the fine roots of asymptomatic and resistant plants [3]. A specific fungicide that can significantly suppress the microsclerotia has yet to identified or approved [1].

Currently, a substantial amount of research is devoted to the use of biocontrol agents (BCAs) to control *Verticillium* wilt [4]. These BCAs may operate by competition, parasitism, the production of antimicrobial compounds (antibiosis), or the induction of resistance (induced systemic resistance, ISR) in the host plant [5]. *Bacillus* species have a long history of use as BCAs in controlling plant disease [6, 7]. These bacteria produce a variety of cyclic lipopeptides (LPs) formed by cyclic peptide structures, including iturins, surfactins, and fengycins [8, 9]. A number of LPs have been shown to induce defense mechanisms and thus, confer indirect protection to the plant [10, 11]. Compounds, such as fengycins, massetolide A, and surfactins, are able to stimulate ISR in bean, wheat, and tomato plants [12–14].

Bacillus species are already used in several commercial biofungicide formulations, such as Serenade® and Kodiak® [15]. They have a long history of study and use for the biological control of plant pathogens [8]. Certainly, biofungicides are not always effective and have proven to be more efficient when applied in the early stages rather than post-infection [16, 17]. Peng [18] previously reported that a biofungicide produced by *Bacillus* is not an effective approach to control clubroot on canola. In addition, we have isolated endophytic *Bacillus* N-4 from *Sophora alopecuroides* plants. After strain screening and testing of volatile antibacterial substances, we have proved that it has a strong inhibitory effect and biocontrol ability against *Verticillium dahliae*.

Fungi respond to environmental changes and when faced with adverse conditions, survive via the activation of resistance pathways. Based on the yeast model, the target of rapamycin (TOR) pathway in *V. dahliae* has been widely studied. The TOR pathway is an evolutionarily conserved phosphoinositide-3 kinase-related kinase (PIKK)-dependent cascade that controls multiple cellular processes in response to various intracellular and extracellular signals [19, 20]. Plants, animals (especially cancer cells), and fungal cells utilize the TOR pathway to thrive under stress [21–23]. The TOR pathway contains two distinct protein complexes: TOR Complexes 1 (TORC1) and 2 (TORC2). TORC2 can phosphorylate PKC1 and participates in the maintenance of cell wall integrity [24]. A primary determining factor of fungal stress resistance is the cell wall. The inhibition of formation of fungal cell walls has been widely studied. The initiation of TORC1 involves many factors, such as growth factors, oxygen, and amino acid levels [25]. TORC2 primarily functions as an effector of insulin/PI3K signaling [26] and an activator associated with the ribosome and growth factors [27].

Mitochondria, as the principal source of production of cellular energy, respond to cellular oxidation levels. They possess an antioxidant defense system that maintains the redox balance [28]. Cells utilize a selective vacuolar degradation process in mitochondria or mitophagy via autophagy-related proteins to degrade and recycle damaged and superfluous mitochondria. It is also possible that mitophagy plays a role in the adaptation to environmental conditions by altering the quality and number of mitochondria [29, 30].

The redox signaling pathway is often utilized to eliminate reactive oxygen species (ROS) induced by UV irradiation, high temperatures, chemical herbicides, and other environmental stressors [31, 32]. The production of ROS is partially responsible for the induction of cell death by *Bacillus* LPs [33], but the fungi can eliminate large amounts of ROS to survive. The levels of expression of genes associated with the oxidative response and the production of superoxide ions (NADPH oxidase) were tested in response to the high concentrations of ROS induced by iturin [34]. The three main systems that play vital roles in removing ROS in cells are 1) Cu- and Zn-superoxide dismutases (SODs), catalase (CAT) or glutathione systems, 2) the peroxiredoxin system, and 3) the thioredoxin system [32].

Moreover, fungal melanin protects both the fungus from fatal radiation and the cell wall from enzymatic activity and can also bind heavy metals, thus, protecting the fungus [35–37]. The *VMK1* gene is a mitogen-activated protein kinase gene, which affects the pathogenicity of *V. dahliae* by affecting the

formation of microsclerotia [38, 39]. Numerous fungi form structures termed sclerotia that are disseminated in infected soil and survive for long periods under stressful environmental conditions. Microsclerotia are required for virulence in *V. dahliae*, and strains that are defective in microsclerotia do not colonize plant roots efficiently or cause disease symptoms [40]. The fungus produces melanized microsclerotia, which assists its survival in adverse environmental conditions in both the soil and hosts. Melanin production in fungi is mediated by two main pathways: the DHN pathway and the L-DOPA pathway [41]. Both pathways are initiated from small molecules and result in melanin synthesis under the action of various enzymes.

Although some progress has been made in the biocontrol of *V. dahliae*, there are few studies on the stress response and self-regulatory mechanism of *V. dahliae* under inhibition by biocontrol bacteria. In this study, we constructed a co-culture system to control the colony size and niche occupancy of *V. dahliae* in the co-culture system by inoculating *Bacillus* at different times. The aim of this study was to explore the self-resistance mechanism of *V. dahliae* under *Bacillus*-induced stress using transcriptome analysis and to provide clues for the control of *Verticillium* wilt disease.

Results

Effect of *Bacillus* N-4 on the *V. dahliae* spores

The spore number and germination rate of *V. dahliae* were determined from the shaking cultures of CK, Gp0, Gp1, Gp2 and Gp3. When co-cultured with N-4, the size of the *V. dahliae* colony increased, the total number of spores, the germination number and germination rate also visibly increased (Fig. 1A-C). Interestingly, although the total number of spores in the treatment group that contained N-4 was always less than that of the CK, the germination rates of Gp3 and Gp2 were higher than that of the CK (Fig. 1B, C). The spore germination rate reflects the degree of inhibition of the fungus. This indicated that larger *V. dahliae* colonies are less inhibited by *Bacillus*.

Antagonism of *Bacillus* N-4 against *V. dahliae*

In vitro confrontation bioassays were conducted for 7 days of culture in Gp0, Gp1, Gp2 and Gp3, and the corresponding strains of *V. dahliae* were designated Vd0, Vd1, Vd2 and Vd3, respectively. Microscopic examination showed that the hyphae in Vd0 were circular and cracked; the microsclerotia were damaged and reduced, and many cells had incomplete cell walls (Fig. 2B). The black microsclerotia could be seen in Vd3 but were barely visible in Vd0 (Fig. 2A). The morphological characteristics of Vd3 were closer to those of the CK.

Analysis of *VMK1* gene expression

Compared with the CK, the expression of *VMK1* gene was downregulated in all of the co-culture groups with the exception of Vd3. When the two strains were co-cultured for 7 days, the difference of expression of *VMK1* gene was the most significant. Therefore, we chose this stage for subsequent RNA-Seq analysis (Fig. 3).

RNA-Seq analysis of *V. dahliae*

Four genes related to the TOR pathway and one gene related to melanin expression were selected to verify the reliability of RNA-Seq. Comparisons of the FPKM and RT-qPCR data showed consistency and correlation between the two datasets (Figure S1).

Nine libraries (three replicates each of the CK, Vd0, and Vd3, covering each of the key time points) were produced by RNA-Seq. Both the abundance of the genes detected and the length of transcripts were deemed sufficient by assessing the number of clean reads obtained in each cDNA library after quality filtering. We obtained an average of 46,240,973 reads per sample (Table 2). In total, 89.37% of the total reads from all nine samples were aligned to the *V. dahliae* genome *(VdLs.17* genome) with < 2 bp mismatches. Mapping analyses revealed that 10,811 of the predicted genes were expressed. Of these, 97.78% were annotated in the database described above (Table S2).

To elucidate the dynamic changes in gene expression in the three experimental groups, the genes that were differentially expressed among the libraries (FDR < 0.05) were identified. Comparisons of gene expression among those groups showed that 144 (116 upregulated and 28 downregulated), 542 (158 upregulated and 384 downregulated), and 18 (15 upregulated and 3 downregulated) genes were significantly differentially expressed between the CK and Vd0, Vd0 and Vd3, and Vd3 and CK, respectively (FDR < 0.05) (Fig. 4A). KEGG enrichment analyses were conducted to explore the potential roles of these DEGs in more detail (Figs. 4B-F). TOR and Mitophagy pathways were significantly enriched (FDR < 0.05) in the 158 genes that were upregulated between Vd0 and Vd3.

The clustering affinity search technique (CAST) and screening of the DEGs were used to generate gene clusters. The expression of gene clusters was identified using the annotation tags in the database and included central metabolism, signaling pathway, transcription factor, biosynthesis of secondary metabolites, ROS scavenger, and cell wall (Fig. 5A-D). It showed that in the larger-scale community of *V. dahliae* in Vd3, the genes involved in glycometabolism and fatty acid degradation were downregulated, while those involved in nitrogen metabolism were more active (Fig. 5A). Signaling pathways that were observed included MAPK, RGS, GPCR, and calcineurin. However, their expression was not significantly different among the three groups (Fig. 5B). Overall, the expression of four transcription factors in CK and Vd3 was similar (Fig. 5C). Gene expression related to secondary metabolism was downregulated in Vd0, while the expression related to ABC transporters was upregulated in Vd3 (Fig. 5D). The genes related to ROS scavenging were generally upregulated in the stress groups (Fig. 5E). The genes related to cell wall formation were upregulated in Vd3, while those that contribute to the degradation of cell walls were upregulated in Vd0 (Fig. 5F).

Analysis of the genes related to scavenging ROS

We observed that the expression of gene clusters related to scavenging ROS was generally higher in the stress group compared with that in the control (Fig. 5E). Therefore, we constructed heat maps of the key gene expression profiles that scavenge ROS (Fig. 6). It is notable that *Prx1* (*VDAG_06751*) was upregulated in Vd3 (Fig. 6H). The stress groups showed markedly higher activity of pyridoxal reductase (*VDAG_03228*, *VDAG_04222*) and pyridoxal kinase (*VDAG_04313*) compared with the control (Fig. 6G). *VDAG_08350* and *VDAG_04529* are putative transcription factors that relate to scavenging ROS, as characterized by the EggNOG and GO databases, and their expression was upregulated in Vd3 to some extent (Fig. 6F).

Analysis of the genes related to microsclerotia formation pathways

We combined the heat maps of some key genes in the formation of microsclerotia with the two main pathways, DHN and L-DOPA, of microsclerotia formation (Fig. 7). The results showed that the *VdCmr1* (*VDAG_01770*) gene in the DHN pathway was upregulated in Vd3, and the *VDAG_03665* gene was significantly upregulated in Vd0 compared with that in the CK. The genes *VDAG_07137* and *VDAG_04798* related to tyrosinase in the L-DOPA pathway were upregulated in vd0, compared with the CK.

Analysis of the genes related to cell wall synthesis

In the phenotypic study conducted above, it was observed from microscopy that the cell wall of Vd3 microsclerotia was thicker, and the cell connection was closer than that in the CK (Fig. 2B). Several important genes related to cell wall synthesis were upregulated in Vd3 (Fig. 8F). These included *VDAG_02340* (1,3-beta-glucan synthase component GLS2), *VDAG_02341* (1,3-beta-glucan synthase component GLS2), and *VDAG_02305* (chitin synthase regulatory factor). *RhoA* (*VDAG_06919*), *PKC1* (*VDAG_09909*), and *BCK1* (*VDAG_00874*) were the key genes in the CWI pathway that were also upregulated in Vd3 (Fig. 8E). We analyzed the expression of genes that are important components of the cell wall, including chitin and glucan. We found that compared with CK, Vd0 expressed more analytic enzymes, while Vd3 expressed more synthetic enzymes (Fig. 5F).

Discussion

The TOR pathway generally plays a role in the regulation of cells in severe environments. Biocontrol bacteria compete with *V. dahliae* for niches and nutrition and release compounds, such as LPs, that inhibit the growth of *V. dahliae*. This pathway should be inhibited in fungi under stress, just as observed in Vd0. However, it was enriched and upregulated in Vd3. Elements upstream of TORC activate the pathway. GATOR2 (Fig. 9B) is a central node in the activation of TORC1 activated by high levels of the

amino acids leucine and arginine [20, 42] with the Rag family of guanosine triphosphatases (GTPases), downstream of GATOR2, promoting the TORC1 response to amino acids [43]. Another upstream element, Rheb, acts as a signal receptor to activate TORC1 through direct interaction [44]. Alternatively, the tuberous sclerosis complex (TSC) and GATOR1 (Fig. 9D) respond to poor growth conditions and inhibit TORC1 [45, 46]. Moreover, PI3K can regulate TORC2 and plays an essential role in the TOR pathway [47]. Overall, the upstream genes that activate TORC were found to be upregulated in Vd3 (Fig. 8C), particularly in the case of GATOR2, which may largely explain the upregulation of TORC. We found that Vd3 may accumulate arginine and leucine or another activator *in vivo* to activate the expression of GATOR2. These results demonstrate that the nutritional status of Vd3 was sufficient, at least compared with that in Vd0.

The mitophagy pathway was also significantly enriched (FDR < 0.05) in the 158 genes that were differentially upregulated between Vd0 and Vd3. In yeast, the ATG family proteins ATG32, ATG11, and ATG8 play unique and vital roles in mitophagy [48]. In addition, the mitophagy pathway plays an integral role in the response to stress. In filamentous fungi, ATG24 is thought to be homologous to ATG32 in yeast [49]. All the ATG proteins were upregulated in Vd3 (Fig. 8G).

Vd0 and Vd3 all bind themselves to scavenging ROS. However, Vd3 was more efficient at scavenging ROS in mitochondria and thus, avoiding mitochondrial-induced apoptosis [50, 51]. Mitochondria may act as the Achilles' heel of fungi [52]. The expression of Aup1, which mediates the regulation of RTG3 to participate in the retrograde signaling pathway (RTG) [53], was also prominently upregulated in Vd3. The RTG signaling-mediated cell response to mitochondrial dysfunction is involved in the enclosed induction of antioxidant defense and stress resistance [54]. Therefore, Vd3 with a larger colony can more effectively utilize the function of mitochondria and avoid damage to itself.

The peroxiredoxin isoform, Prx1, which is found in mitochondria and acts as a ROS scavenger, was significantly upregulated in Vd3. A recent study showed that high levels of Prx1 expression are related to niche adaptation [55] (Fig. 6H). Peroxiredoxins are key intermediates in removing ROS and quantitatively are the most abundant cellular redox defense. In yeast, there are five isoforms encoded by independent genes, with AHP1, TSA1, and TSA2 found in the cytoplasm, Dot5 in the nucleus, and Prx1 in the mitochondria. The larger colonies (Vd3) appeared to be more effective at expressing pyridoxal kinase to produce pyridoxal phosphate, which is an active form of vitamin B6. Additionally, vitamin B6 (pyridoxine) and its derivatives are also efficient at removing ROS [56]. Lastly, we explored the response of transcription factors to the ROS (Fig. 6F). The activator protein 1 (AP-1) transcription factor governs the low level defense response to oxidative stress and is responsible for regulating the transcription of various genes involved in ROS detoxification [57]. *VdSkn7* plays a key role in microsclerotial development and stress resistance [58].

VdCmr1 (VDAG_01770), a key transcription factor that regulates melanin synthesis associated with the DHN pathway [59] was found to be upregulated in Vd3 (Fig. 7). Other genes involved in microsclerotia formation (e.g., *VdCrz1, VdMsb2*, and *VdMsn2*) [60–62] did not show differential expression among the three stress groups (Fig. S2). In this study, the Vd3 with a larger colony adopted more effective strategies

to attain better resistance. We found that maintaining the integrity of the cell wall is advantageous over melanin synthesis under the stress induced by *Bacillus* or LPs, since melanin is not essential for microsclerotia development. Bell had previously found genetic mutants of *V. dahliae* that can produce microsclerotia without pigmentation [63]. Moreover, melanin granules are deposited within the cell walls and between the cells, cross-linking with components of the cell wall, such as chitin [64, 65]. In our study, although the genes directly involved in melanin production were significantly upregulated in Vd0, the number of microsclerotia did not increase. Observations of the microsclerotia morphology revealed that the cell walls in Vd0 were damaged (Fig. 3B). Other than in Vd0, the cell wall in Vd3 was stronger, and the expression of melanin synthesis genes was similar to that of the CK. More importantly, the key transcription factor VdCmr1 was significantly upregulated. This study found that in VD3, the TOR and CWI pathways were significantly enriched in the upregulated genes related to cell wall synthesis (Fig. 8). This indicates that the TOR pathway plays a potential role in the structural enhancement of Vd3 cell wall. The CWI pathway is the primary signaling pathway that is responsible for the regulation of cell wall stress responses and also participates in the transduction of other stimuli, such as oxidative and genotoxic stressors [66, 67]. In summary, both the TOR and CWI pathways played vital roles in strengthening the cell wall of Vd3. Therefore, our study shows that under stress conditions, *V. dahliae* can ensure the functional integrity of its cell wall by upregulating the genes related to cell wall synthesis. The cell wall plays an important role in the production of micronuclei of *V. dahliae*.

This study did not seek to overturn the potential of biocontrol bacteria as a new era of biological control pathogens. *Bacillus* strain N-4 was selected for isolation owing to its excellent ability to inhibit *V. dahliae*. Extensive research has shown that *Bacillus* spp. or their LPs can influence the secretion of chitinase and glucanase, damage biological membranes, suppress spore germination and mycelial growth, and ruin the formation of microsclerotia in *V. dahliae* [68–71]. Nevertheless, these studies were not focused on fungal colonies, but on dispersed fungal spores in culture media with added bacterial fermentation liquid or directly added biocontrol bacteria for co-culture. These approaches did not enable the formation of *V. dahliae* colonies characterized by the direct communication of hyphae that is indicative of colony structure.

In our study, we determined that a larger colony of *V. dahliae* could survive the stress of biocontrol bacteria. In fact, the aggregation of pathogenic fungi on plant is inevitable. For example, the gray mold caused by *Botrytis cinerea* can form infection cushions during penetration [72]. According to observations in the early stage of this experiment, the CK generally produced microsclerotia that were visible to the naked eye approximately 5 days after inoculation. Therefore, the reason for the resistance of Vd3 could be that it entered a more resistant stage earlier than Vd0. For example, it produced microsclerotia earlier. Therefore, the prevention of diseases is often more effective than treating active ones. The optimal effect can be achieved by the balanced application of biofungicides. In this process, the focus must be on the mechanism of fungal resistance. This result can provide insight into the prevention and treatment of *Verticillium* wilt and other diseases caused by fungi in agricultural production.

Conclusions

This study showed that larger colonies of *V. dahliae* were less inhibited by *Bacillus*. When faced with biocontrol bacteria, larger colonies can regulate the TOR pathway, cell wall synthesis, microsclerotia formation, and scavenge ROS, so as to preserve homeostasis *in vivo* and more effectively participate in niche competition. This study was based on the antagonistic effect of *Bacillus* on *V. dahliae* and revealed the self-regulatory mechanism of *V. dahliae* after inhibition by transcriptome analysis. This can explain why treatment using microbial agents can sometimes be ineffective and suggests that the prevention of *Verticillium* wilt by *Bacillus* is more effective than the treatment.

Methods

Microbial materials and culture conditions

Bacillus strain N-4 (*Bacillus* spp.) was isolated from *Sophora alopecuroides* and preserved in the Key Laboratory of Agricultural Biotechnology, Shihezi University, Xinjiang, China. The strain was cultured continuously in Luria-Bertani broth (LB) at 30°C for 2 days, and single colonies were obtained on LB agar using the spread plate method.

V. dahliae strain VdSHZ-9 (a defoliating pathotype) was isolated from cotton soil infected with *Verticillium* wilt in Shihezi, Xinjiang, China. The strain was cultured on potato dextrose agar (PDA) at 25°C in the dark. Strains of *V. dahliae* were inoculated into potato dextrose broth (PDB) and cultured at 25°C and 180 rpm in the dark for 3 days. Subsequently, the spore suspension was diluted to approximately 10^{-6}, and single colonies were obtained on PDA agar plates. A single colony was inoculated into a new PDA petri dish for cultivation in the future.

Dual culture method of strains

First, 8 mm diameter mycelial discs from *V. dahliae* isolates were placed on 9 cm PDA plates and cultured at 25℃ in the dark. On days 0, 1, 2 and 3 days of culture, B*acillus N-4* was inoculated in four diagonal directions, which were 3 cm away from the mycelial disc. According to the time of inoculation of *Bacillus N-4*, the co-cultured groups were designated Gp0, Gp1, Gp2 and Gp3 (Table 1). The CK group was inoculated with a *V. dahliae* mycelial disc at the beginning but was not treated with *Bacillus*. All the groups continued their culture at 25℃ in the dark with 10 replicates per group.

Effect of *Bacillus* N-4 on *V. dahliae* spores

On days 5 to 10 of the co-culture of fungi and bacteria in each group and days 5 to 13 of the CK culture, a mycelial disc 8 mm in diameter was taken from the edge of the colony of *V. dahliae* and inoculated into PDB each day. A suspension of spores was obtained after 4 days of culture at 25℃ and 180 rpm (Table

1). The spore suspension was diluted 100-fold and counted with a hemocytometer. The average value was taken as the number of spores. In addition, the spore suspension was diluted to 10^{-5}, 10^{-6}, and 10^{-7}, respectively, and then cultured on PDA to obtain a single colony and counted. The average value was the number of germinated spores. The percentage of germination was calculated as follows:

percent germination(%) = 100 × (germinated spores)/(total spores

Antagonism of *Bacillus* N-4 against *V. dahliae*

On day 7 of the co-culture of bacteria and fungi from the Gp0 and Gp3 groups, the front and back sides of the petri dish were photographed to record the colony morphology. To stay consistent with the culture time of *V. dahliae* in Gp3, the CK was photographed on day 10 (Table 1). Hyphae and microsclerotia were collected from the *V. dahliae* colony, placed on a glass slide that contained sterile water, covered with a coverslip which was tapped slightly to ensure dispersion, and observed under a light microscope.

Determination of *VMK1* gene expression

On days 5 to 10 of the co-culture of fungi and bacteria in each group and days 8 to 13 of the CK culture, a mycelial disc 8 mm in diameter was taken from the edge of the colony of *V. dahliae* and inoculated into PDB each day. A spore suspension was obtained after 7 days of culture at 25℃ and 180 rpm. This period of growth enabled the fungus to accumulate enough biomass that RNA could be extracted (Table 1). *V. dahliae* was then ground to a fine powder in liquid nitrogen using a mortar and pestle. The total RNA was extracted using an EZgene™ Fungal RNA Lit (Biomiga, Shanghai, China). After elution in RNase-free water, the RNA was stored at −80°C until further use.

Total RNA was used for the first-strand cDNA synthesis using a RevertAid™ First Strand cDNA Synthesis Kit (Thermo Scientific, (EU) Lithuania), according to the manufacturer's instructions. Quantitative real-time PCR (qRT-PCR) was performed on a Light Cycler 480 system (Roche Diagnostics, Penzberg, Germany) using the Light Cycler 480 SYBR Green master mix (Roche Diagnostics). The internal reference for the qRT-PCR was the *V. dahliae* β-tubulin gene (*VDAG_10074*) The 2^{-rrt} method [73] was used to calculate the relative gene expression. The experiment had three operational and three biological repetitions. Primer designing tools (https://www.ncbi.nlm.nih.gov/tools/primer-blast/) (Table S1) were used to design the primers. To determine the correlation between transcriptome sequencing and qRT-PCR, a Pearson coefficient was calculated using R software version 3.5 (BGI, Beijing, China).

RNA-Seq of *V. dahliae*

The library was constructed using an Illumina TruSeq™ RNA Sample Prep Kit according to the manufacturer's instructions and run on an Illumina NovaSeq 6000 platform (Illumina, San Diego, CA,

USA). Following sequencing by Majorbio, Inc. (Shanghai, China), dirty reads were separated from the high-quality clean reads by removing the reads that contained two or more Ns and low-quality reads with adaptors or two Ns. Clean reads from each sample were mapped to the *V. dahliae VdLs.17* genome (https://www.ncbi.nlm.nih.gov/bioproject/PRJNA28529) using TopHat [74] to predict the exon splice sites allowing < two mismatches. The DESeq Bioconductor package [75] was used to normalize the mapped reads. The sequences of genes and transcripts were compared using Diamond software [76] in three databases: NR (NCBI non-redundant protein sequences, using e-value = $1e^{-5}$), Swiss-Prot (using e-value = $1e^{-5}$), and EggNOG (evolutionary genealogy of genes: Non-supervised Orthologous Groups, using e-value =$1e^{-5}$). The GO annotations were used in Blast2GO [77], Pfam annotations were used in Hmmer [78], and KEGG annotations were used in KOBAS2.1 [79], all with e-values equal to $1e^{-5}$.

Analysis of differentially expressed genes

FPKM (fragments per kilobase of transcript per million mapped fragments) in Cufflinks [80] were used to calculate the levels of gene expression. The edgeR program [81] was used to determine the differentially expressed genes (DEGs) between the samples, using the standards of adjusted P-value ≤0.05 and fold change ≥1.5 or ≤ 0.67. Goatools [82] was used to analyze the GO enrichment of the DEGs, while KEGG pathway analysis was performed with KOBAS software [83].

Abbreviations

PDA: Potato dextrose aga

PDB: Potato dextrose broth

LPs: Lipopeptides

BCAs: Biocontrol agents

DEGs: Differentially expressed genes

TOR: Target of rapamycin pathways

ROS: Reactive oxygen species

Declarations

Availability of data and materials

The RNA-Seq data were submitted to the NCBI SRA database (http://www.ncbi.nlm.nih.gov/Traces/sra/) with the accession numbers: SRR10963691, SRR10963690, SRR10963689, SRR10963688,

SRR10963687, SRR10963686, SRR10963685, SRR10963684, SRR10963683.The datasets used and/or analysed during the current study are available from the corresponding author on reasonable request.

Funding

This research was funded by Genetically Modified Major Project (2018ZX0800501B-005) and National College Students Innovation and Entrepreneurship Training Program (201810759074).

Author information

Wenhui Tian and Zhenrui Cheng contributed equally to this work.

Affiliations

College of Life Science, University of Shihezi, Shihezi, China.

Wenhui Tian, Zhenrui Cheng, Junxia Wang, Fengfeng Cheng, Luping Li, Chunxiao Huo, Wenxuan Li, Shouyan Han, Xinyong Guo, Aiying Wang

Contributions

WT, ZC, FC and AW designed the experiment. JW, CH and SH collect and process samples. WT, ZC, LL and WL performed the experiment. ZC and XG analyzed the data. WT and ZC wrote the manuscript. All authors have read and approved the final version of the manuscript.

Corresponding authors

Correspondence to Aiying Wang.

References

1. Klosterman SJ, Atallah ZK, Vallad GE, Subbarao KV: **Diversity, Pathogenicity, and Management of Verticillium Species**. *Annual Review of Phytopathology* 2009, **47**(1):39-62.

2. Fradin EF, Thomma BPHJ: **Physiology and molecular aspects of Verticillium wilt diseases caused by V. dahliae and V. albo-atrum**. *Molecular Plant Pathology* 2006, **7**(2):71-86.

3. Xiao CL, Subbarao KV, Schulbach KF, Koike ST: **Effects of crop rotation and irrigation on Verticillium dahliae microsclerotia in soil and wilt in cauliflower**. *Phytopathology* 1998, **88**(10):1046-1055.

4. Perez-Garcia A, Romero D, de Vicente A: **Plant protection and growth stimulation by microorganisms: biotechnological applications of Bacilli in agriculture**. *Curr Opin Biotechnol* 2011, **22**(2):187-193.

5. Ongena M, Jacques P, Touré Y, Destain J, Jabrane A, Thonart P: **Involvement of fengycin-type lipopeptides in the multifaceted biocontrol potential of Bacillus subtilis**. *Applied Microbiology and Biotechnology* 2005, **69**(1):29-38.

6. Abbas A, Khan SU, Khan WU, Saleh TA, Khan MHU, Ullah S, Ali A, Ikram M: **Antagonist effects of strains of Bacillus spp. against Rhizoctonia solani for their protection against several plant diseases: Alternatives to chemical pesticides**. *C R Biol* 2019, **342**(5-6):124-135.

7. Nguvo KJ, Gao X: **Weapons hidden underneath: bio-control agents and their potentials to activate plant induced systemic resistance in controlling crop Fusarium diseases**. *Journal of Plant Diseases and Protection* 2019, **126**(3):177-190.

8. Ongena M, Jacques P: **Bacillus lipopeptides: versatile weapons for plant disease biocontrol**. *Trends in Microbiology* 2008, **16**(3):115-125.

9. Kaspar F, Neubauer P, Gimpel M: **Bioactive Secondary Metabolites from Bacillus subtilis: A Comprehensive Review**. *Journal of Natural Products* 2019, **82**(7):2038-2053.

10. Choudhary DK, Johri BN: **Interactions of Bacillus spp. and plants–with special reference to induced systemic resistance (ISR)**. *Microbiol Res* 2009, **164**(5):493-513.

11. Tunsagool P, Jutidamrongphan W, Phaonakrop N, Jaresitthikunchai J, Roytrakul S, Leelasuphakul W: **Insights into stress responses in mandarins triggered by Bacillus subtilis cyclic lipopeptides and exogenous plant hormones upon Penicillium digitatum infection**. *Plant Cell Reports* 2019, **38**(5):559-575.

12. Ongena M, Jourdan E, Adam A, Paquot M, Brans A, Joris B, Arpigny J-L, Thonart P: **Surfactin and fengycin lipopeptides of Bacillus subtilis as elicitors of induced systemic resistance in plants**. *Environmental microbiology* 2007, **9**:1084-1090.

13. Tran H, Ficke A, Asiimwe T, Hofte M, Raaijmakers JM: **Role of the cyclic lipopeptide massetolide A in biological control of Phytophthora infestans and in colonization of tomato plants by Pseudomonas fluorescens**. *New Phytologist* 2007, **175**(4):731-742.

14. Khong NG, Randoux B, Deravel J, Tisserant B, Tayeh C, Coutte F, Bourdon N, Jacques P, Reignault P: **Induction of resistance in wheat by bacterial cyclic lipopeptides**. *Communications in agricultural and applied biological sciences* 2013, **78**(3):479-487.

15. Falardeau J, Wise C, Novitsky L, Avis TJ: **Ecological and Mechanistic Insights Into the Direct and Indirect Antimicrobial Properties of Bacillus subtilis Lipopeptides on Plant Pathogens**. *Journal of Chemical Ecology* 2013, **39**(7):869-878.

16. Matzen N, Heick TM, Jorgensen LN: **Control of powdery mildew (Blumeria graminis spp.) in cereals by Serenade (R) ASO (Bacillus amyloliquefaciens (former subtilis) strain QST 713)**. *Biol Control* 2019, **139**:8.

17. Rekanovic E, Milijašević-Marčić S, Todorovic B, Potocnik I: **Possibilities of biological and chemical control of Verticillium wilt in pepper**. *Phytoparasitica* 2007, **35**:436-441.

18. Peng G, Pageau D, Strelkov S, Lahlali R, Hwang S, Hynes R, Anderson K, McDonald MR, Bd G, Turkington T *et al*: **Assessment of crop rotation, cultivar resistance and Bacillus subtilis biofungicide for clubroot on canola**. *Acta horticulturae* 2013, **1005**:591-598.

19. Dobrenel T, Caldana C, Hanson J, Robaglia C, Vincentz M, Veit B, Meyer C: **TOR Signaling and Nutrient Sensing**. *Annual Review of Plant Biology* 2016, **67**(1):261-285.

20. Saxton RA, Sabatini DM: **mTOR Signaling in Growth, Metabolism, and Disease**. *Cell* 2017, **168**(6):960-976.

21. Beuvink I, Boulay A, Fumagalli S, Zilbermann F, Ruetz S, O'Reilly T, Natt F, Hall J, Lane HA, Thomas G: **The mTOR Inhibitor RAD001 Sensitizes Tumor Cells to DNA-Damaged Induced Apoptosis through Inhibition of p21 Translation**. *Cell* 2005, **120**(6):747-759.

22. Deprost D, Yao L, Sormani R, Moreau M, Leterreux G, Nicolai M, Bedu M, Robaglia C, Meyer C: **The Arabidopsis TOR kinase links plant growth, yield, stress resistance and mRNA translation**. *EMBO Rep* 2007, **8**(9):864-870.

23. He Z, Zhao X, Lu Z, Wang H, Liu P, Zeng F, Zhang Y: **Comparative transcriptome and gene co-expression network analysis reveal genes and signaling pathways adaptively responsive to varied adverse stresses in the insect fungal pathogen, Beauveria bassiana**. *Journal of Invertebrate Pathology* 2018, **151**:169-181.

24. Nomura W, Inoue Y: **Methylglyoxal activates the target of rapamycin complex 2-protein kinase C signaling pathway in Saccharomyces cerevisiae**. *Mol Cell Biol* 2015, **35**(7):1269-1280.

25. Laplante M, Sabatini DM: **mTOR signaling at a glance**. *Journal of Cell Science* 2009, **122**(20):3589-3594.

26. Loewith R, Jacinto E, Wullschleger S, Lorberg A, Crespo JL, Bonenfant D, Oppliger W, Jenoe P, Hall MN: **Two TOR Complexes, Only One of which Is Rapamycin Sensitive, Have Distinct Roles in Cell Growth Control**. *Molecular Cell* 2002, **10**(3):457-468.

27. Xie X, Guan KL: **The ribosome and TORC2: collaborators for cell growth**. *Cell* 2011, **144**(5):640-642.

28. Czarna M, Jarmuszkiewicz W: **Role of mitochondria in reactive oxygen species generation and removal; relevance to signaling and programmed cell death**. *Postepy biochemii* 2006, **52**(2):145-156.

29. Bhatia-Kiššová I, Camougrand N: **Mitophagy in yeast: actors and physiological roles**. *FEMS Yeast Research* 2010, **10**(8):1023-1034.

30. Scheckhuber CQ, Hamann A, Brust D, Osiewacz HD: **Cellular Homeostasis in Fungi: Impact on the Aging Process**. In: *Aging Research in Yeast.* Edited by Breitenbach M, Jazwinski SM, Laun P. Dordrecht: Springer Netherlands; 2012: 233-250.

31. Zhang LB, Feng MG: **Antioxidant enzymes and their contributions to biological control potential of fungal insect pathogens**. *Appl Microbiol Biotechnol* 2018, **102**(12):4995-5004.

32. Breitenbach M, Weber M, Rinnerthaler M, Karl T, Breitenbach-Koller L: **Oxidative stress in fungi: its function in signal transduction, interaction with plant hosts, and lignocellulose degradation**. *Biomolecules* 2015, **5**(2):318-342.

33. Cao X-h, Zhao S-s, Liu D-y, Wang Z, Niu L-l, Hou L-h, Wang C-l: **ROS-Ca2+ is associated with mitochondria permeability transition pore involved in surfactin-induced MCF-7 cells apoptosis**. *Chemico-Biological Interactions* 2011, **190**(1):16-27.

34. Han Q, Wu F, Wang X, Qi H, Shi L, Ren A, Liu Q, Zhao M, Tang C: **The bacterial lipopeptide iturins induce Verticillium dahliae cell death by affecting fungal signalling pathways and mediate plant defence responses involved in pathogen-associated molecular pattern-triggered immunity**. *Environmental Microbiology* 2015, **17**(4):1166-1188.

35. Dadachova E, Casadevall A: **Ionizing radiation: how fungi cope, adapt, and exploit with the help of melanin**. *Current Opinion in Microbiology* 2008, **11**(6):525-531.

36. Schultzhaus Z, Chen A, Kim S, Shuryak I, Chang M, Wang Z: **Transcriptomic analysis reveals the relationship of melanization to growth and resistance to gamma radiation in Cryptococcus neoformans**. *Environmental Microbiology* 2019, **21**(8):2613-2628.

37. Pihet M, Vandeputte P, Tronchin G, Renier G, Saulnier P, Georgeault S, Mallet R, Chabasse D, Symoens F, Bouchara J: **Melanin is an essential component for the integrity of the cell wall of Aspergillus fumigatus conidia**. *BMC Microbiology* 2009, **9**(1):177-177.

38. P SP, BP TBPHJ: **Verticillium dahliae Sge1 differentially regulates expression of candidate effector genes.**, vol. 26; 2013.

39. Tran VT, Braus-Stromeyer SA, Kusch H, Reusche M, Kaever A, Kuhn A, Valerius O, Landesfeind M, Asshauer K, Tech M *et al*: **Verticillium transcription activator of adhesion Vta2 suppresses microsclerotia formation and is required for systemic infection of plant roots**. *New Phytol* 2014, **202**(2):565-581.

40. Xiong D, Wang Y, Tian L, Tian C: **MADS-Box Transcription Factor VdMcm1 Regulates Conidiation, Microsclerotia Formation, Pathogenicity, and Secondary Metabolism of Verticillium dahliae**. *Front Microbiol* 2016, **7**:1192.

41. Eisenman HC, Casadevall A: **Synthesis and assembly of fungal melanin**. *Appl Microbiol Biotechnol* 2012, **93**(3):931-940.

42. Barpeled L, Chantranupong L, Cherniack AD, Chen WW, Ottina K, Grabiner BC, Spear E, Carter SL, Meyerson M, Sabatini DM: **A tumor suppressor complex with GAP activity for the Rag GTPases that signal amino acid sufficiency to mTORC1**. *Science* 2013, **340**(6136):1100-1106.

43. Kim E, Goraksha-Hicks P, Li L, Neufeld TP, Guan K-L: **Regulation of TORC1 by Rag GTPases in nutrient response**. *Nature cell biology* 2008, **10**(8):935-945.

44. Long X, Lin Y, Ortiz-Vega S, Yonezawa K, Avruch J: **Rheb binds and regulates the mTOR kinase**. *Curr Biol* 2005, **15**(8):702-713.

45. Dibble CC, Elis W, Menon S, Qin W, Klekota J, Asara JM, Finan PM, Kwiatkowski DJ, Murphy LO, Manning BD: **TBC1D7 is a third subunit of the TSC1-TSC2 complex upstream of mTORC1**. *Mol Cell* 2012, **47**(4):535-546.

46. Parmigiani A, Nourbakhsh A, Ding B, Wang W, Kim YC, Akopiants K, Guan KL, Karin M, Budanov AV: **Sestrins inhibit mTORC1 kinase activation through the GATOR complex**. *Cell Rep* 2014, **9**(4):1281-1291.

47. Oh WJ, Jacinto E: **mTOR complex 2 signaling and functions**. *Cell Cycle* 2014, **10**(14):2305-2316.

48. Okamoto K, Kondo-Okamoto N, Ohsumi Y: **Mitochondria-Anchored Receptor Atg32 Mediates Degradation of Mitochondria via Selective Autophagy**. *Developmental Cell* 2009, **17**(1):87-97.

49. He Y, Deng YZ, Naqvi NI: **Atg24-assisted mitophagy in the foot cells is necessary for proper asexual differentiation in Magnaporthe oryzae**. *Autophagy* 2013, **9**(11):1818-1827.

50. Chabrier-Rosello Y, Foster TH, Mitra S, Haidaris CG: **Respiratory deficiency enhances the sensitivity of the pathogenic fungus Candida to photodynamic treatment**. *Photochemistry and Photobiology* 2008, **84**(5):1141-1148.

51. Ankarcrona M, Dypbukt JM, Bonfoco E, Zhivotovsky B, Orrenius S, Lipton SA, Nicotera P: **Glutamate-induced neuronal death: A succession of necrosis or apoptosis depending on mitochondrial function**. *Neuron* 1995, **15**(4):961-973.

52. Chatre L, Ricchetti M: **Are mitochondria the Achilles' heel of the Kingdom Fungi?** *Current Opinion in Microbiology* 2014, **20**:49-54.

53. Journo D, Mor A, Abeliovich H: **Aup1-mediated Regulation of Rtg3 during Mitophagy**. *Journal of Biological Chemistry* 2009, **284**(51):35885-35895.

54. Torelli NQ, Ferreira-Júnior JR, Kowaltowski AJ, da Cunha FM: **RTG1- and RTG2-dependent retrograde signaling controls mitochondrial activity and stress resistance in Saccharomyces cerevisiae**. *Free Radical*

Biology and Medicine 2015, **81**:30-37.

55. Jiménez-Ruiz J, Leyva-Pérez MdlO, Gómez-Lama Cabanás C, Barroso JB, Luque F, Mercado-Blanco J: **The Transcriptome of Verticillium dahliae Responds Differentially Depending on the Disease Susceptibility Level of the Olive (Olea europaea L.) Cultivar**. *Genes* 2019, **10**(4):251.

56. Bilski P, Li M, Ehrenshaft M, Daub ME, Chignell CF: **Vitamin B6 (pyridoxine) and its derivatives are efficient singlet oxygen quenchers and potential fungal antioxidants**. *Photochemistry and Photobiology* 2007, **71**(2):129-134.

57. Vivancos A, Castillo EA, Biteau B, Nicot C, Ayte J, Toledano MB, Hidalgo E: **A cysteine-sulfinic acid in peroxiredoxin regulates H2O2-sensing by the antioxidant Pap1 pathway**. *Proceedings of the National Academy of Sciences of the United States of America* 2005, **102**(25):8875-8880.

58. Tang C, Xiong D, Fang Y, Tian C, Wang Y: **The two-component response regulator VdSkn7 plays key roles in microsclerotial development, stress resistance and virulence of Verticillium dahliae**. *Fungal Genet Biol* 2017, **108**:26-35.

59. Wang Y, Hu X, Fang Y, Anchieta A, Goldman PH, Hernandez G, Klosterman SJ: **Transcription factor VdCmr1 is required for pigment production, protection from UV irradiation, and regulates expression of melanin biosynthetic genes in Verticillium dahliae**. *Microbiology* 2018, **164**(4):685-696.

60. Tian L, Xu J, Zhou L, Guo W: **VdMsb regulates virulence and microsclerotia production in the fungal plant pathogen Verticillium dahliae**. *Gene* 2014, **550**(2):238-244.

61. Xiong D, Wang Y, Tang C, Fang Y, Zou J, Tian C: **VdCrz1 is involved in microsclerotia formation and required for full virulence in Verticillium dahliae**. *Fungal Genetics and Biology* 2015, **82**:201-212.

62. Tian L, Yu J, Wang Y, Tian C: **The C2H2 transcription factor VdMsn2 controls hyphal growth, microsclerotia formation, and virulence of Verticillium dahliae**. *Fungal Biol* 2017, **121**(12):1001-1010.

63. A A Bell a, Wheeler MH: **Biosynthesis and Functions of Fungal Melanins**. *Annual Review of Phytopathology* 1986, **24**(1):411-451.

64. Baker LG, Specht CA, Donlin MJ, Lodge JK: **Chitosan, the Deacetylated Form of Chitin, Is Necessary for Cell Wall Integrity inCryptococcus neoformans**. *Eukaryotic Cell* 2007, **6**(5):855-867.

65. Walker CA, Gómez BL, Mora-Montes HM, Mackenzie KS, Munro CA, Brown AJP, Gow NAR, Kibbler CC, Odds FC: **Melanin Externalization in Candida albicans Depends on Cell Wall Chitin Structures**. *Eukaryotic Cell* 2010, **9**(9):1329-1342.

66. Arroyo J, Bermejo C, Garcia R, Rodriguezpena JM: **Genomics in the detection of damage in microbial systems: cell wall stress in yeast**. *Clinical Microbiology and Infection* 2009, **15**:44-46.

67. Jimenez-Gutierrez E, Alegria-Carrasco E, Sellers-Moya A, Molina M, Martin H: **Not just the wall: the other ways to turn the yeast CWI pathway on**. *Int Microbiol* 2020, **23**(1):107-119.

68. Raaijmakers JM, De Bruijn I, Nybroe O, Ongena M: **Natural functions of lipopeptides from Bacillus and Pseudomonas: more than surfactants and antibiotics**. *FEMS Microbiol Rev* 2010, **34**(6):1037-1062.

69. Han Q, Wu F, Wang X, Qi H, Shi L, Ren A, Liu Q, Zhao M, Tang C: **The bacterial lipopeptide iturins induce Verticillium dahliae cell death by affecting fungal signalling pathways and mediate plant defence responses involved in pathogen-associated molecular pattern-triggered immunity**. *Environ Microbiol* 2015, **17**(4):1166-1188.

70. DeFilippi S, Groulx E, Megalla M, Mohamed R, Avis TJ: **Fungal Competitors Affect Production of Antimicrobial Lipopeptides in Bacillus subtilis Strain B9-5**. *J Chem Ecol* 2018, **44**(4):374-383.

71. Yu D, Fang Y, Tang C, Klosterman SJ, Tian C, Wang Y: **Genome-wide transcriptome profiles reveal how Bacillus subtilis lipopeptides inhibit microsclerotia formation in Verticillium dahliae**. *Mol Plant Microbe Interact* 2018.

72. Doehlemann G, Okmen B, Zhu W, Sharon A: **Plant Pathogenic Fungi**. *Microbiol Spectr* 2017, **5**(1).

73. Livak KJ, Schmittgen TD: **Analysis of Relative Gene Expression Data Using Real-Time Quantitative PCR and the 2−ΔΔCT Method**. *Methods* 2001, **25**(4):402-408.

74. Trapnell C, Roberts A, Goff LA, Pertea G, Kim D, Kelley DR, Pimentel H, Salzberg SL, Rinn JL, Pachter L: **Differential gene and transcript expression analysis of RNA-seq experiments with TopHat and Cufflinks**. *Nature Protocols* 2012, **7**(3):562-578.

75. Anders S, Huber W: **Differential expression analysis for sequence count data**. *Genome Biology* 2010, **11**(10):1-12.

76. Buchfink B, Xie C, Huson DH: **Fast and sensitive protein alignment using DIAMOND**. *Nature Methods* 2015, **12**(1):59-60.

77. Conesa A, Gotz S, Garciagomez JM, Terol J, Talon M, Robles M: **Blast2GO: a universal tool for annotation, visualization and analysis in functional genomics research**. *Bioinformatics* 2005, **21**(18):3674-3676.

78. Soding J: **Protein homology detection by HMM-HMM comparison**. *Bioinformatics* 2005, **21**(7):951-960.

79. Xie C, Mao XZ, Huang JJ, Ding Y, Wu JM, Dong S, Kong L, Gao G, Li CY, Wei LP: **KOBAS 2.0: a web server for annotation and identification of enriched pathways and diseases**. *Nucleic Acids Res* 2011, **39**:W316-W322.

80. Trapnell C, Roberts A, Goff L, Pertea G, Kim D, Kelley DR, Pimentel H, Salzberg SL, Rinn JL, Pachter L: **Differential gene and transcript expression analysis of RNA-seq experiments with TopHat and Cufflinks**. *Nature Protocols* 2012, **7**(3):562-578.

81. Robinson MD, Mccarthy DJ, Smyth GK: **edgeR: a Bioconductor package for differential expression analysis of digital gene expression data**. *Bioinformatics* 2010, **26**(1):139-140.

82. Klopfenstein DV, Zhang L, Pedersen BS, Ramirez F, Vesztrocy AW, Naldi A, Mungall CJ, Yunes JM, Botvinnik O, Weigel M: **GOATOOLS: A Python library for Gene Ontology analyses**. *Scientific Reports* 2018, **8**(1):10872.

83. Mao X, Cai T, Olyarchuk JG, Wei L: **Automated genome annotation and pathway identification using the KEGG Orthology (KO) as a controlled vocabulary**. *Bioinformatics* 2005, **21**(19):3787-3793.

84. Howlett BJ, Soanes DM, Chakrabarti A, Paszkiewicz KH, Dawe AL, Talbot NJ: **Genome-wide Transcriptional Profiling of Appressorium Development by the Rice Blast Fungus Magnaporthe oryzae**. *PLoS Pathogens* 2012, **8**(2):e1002514.

Tables

Table 1 The timetable for five groups of experiments.

Day	0	1	2	3	4	5	6	7	8	9	10	11	12	13
Control	>					_	_	_	q	q	p/q/O	q	q	q
Gp3	>			<					q	q	p/q/O	q	q	q
Gp2	>		<					q	q	q	q	q	q	
Gp1	>	<					q	q	q	q	q	q		
Gp0	> <				_	q	q	p/q/O	q	q	q			

The symbol '>' represents the inoculated *V. dahliae*. The symbol '<' represents the inoculated *Bacillus* spp. The symbol '_' represents the determination of spore viability. The abbreviation q represents qRT-PCR. The abbreviation p represents the photo taken, and the O represents the RNA-Seq sampling time. qRT-PCR, quantitative real-time PCR

Table 2 RNA-Seq statistics

Sample	Raw reads[a]	Clean reads[b]	Clean reads Q30 (%)[c]	GC content (%)[d]	Total mapped Ratio (%)[e]	Uniquely mapped Ratio (%)[f]
CK_1	53402662	52487656(98.29%)	91.92	58.66	90.93%	90.39%
CK_2	48965020	47951876(97.93%)	91.1	58.72	90.13%	89.57%
CK_3	44868052	44028970(98.13%)	91.63	58.71	90.51%	89.88%
Vd0_1	47571948	46398134(97.53%)	91.55	58.62	88.68%	87.9%
Vd0_2	45889880	45075930(98.23%)	91.99	58.51	90.1%	89.53%
Vd0_3	45459836	44336540(97.53%)	90.96	58.58	89.16%	88.52%
Vd3_1	47038694	46142234(98.09%)	92.2	58.6	89.92%	89.3%
Vd3_2	48649032	47859358(98.38%)	92.06	58.4	90.31%	89.68%
Vd3_3	42647032	41888066(98.22%)	92.1	58.54	90.2%	89.52%

[a]Number of reads generated from the Illumina NovaSeq 6000.

[b]Raw data with low-quality reads, reads containing 3’ adaptors, and reads containing two or more N bases removed.

[c]The percentage of bases with a mass value over 30.

[d]The GC content of each sample.

[e]The number of reads mapped to the reference genome within 2 bp mismatch.

[f]Uniquely mapped: The number of reads mapped to the reference genome with unique sequence location.

Figures

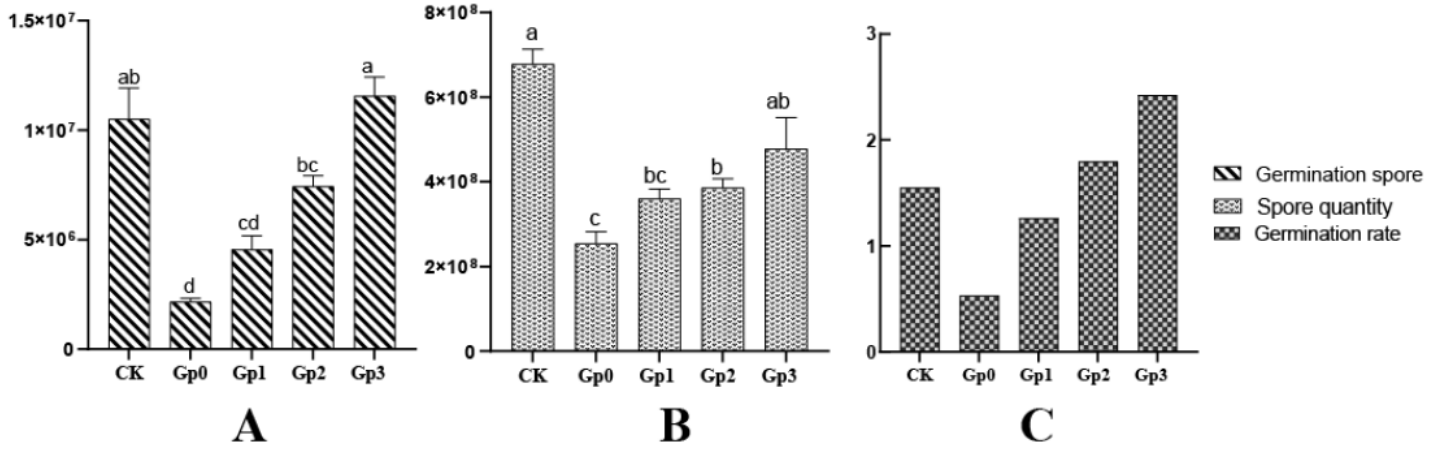

Figure 1

The spore quantity (A), germination quantity (B), and germination rate (%) (C) of the CK, Gp0, Gp1, Gp2 and Gp3. A and B representing the mean ± SEM were subjected to a one-way analysis of variance (ANOVA) with Dunnett's T3 test as post hoc using SPSS version 17.0 program for Windows (http://www.spss.com/). Differences with $P < 0.05$ were considered significant. SEM, standard error of the mean.

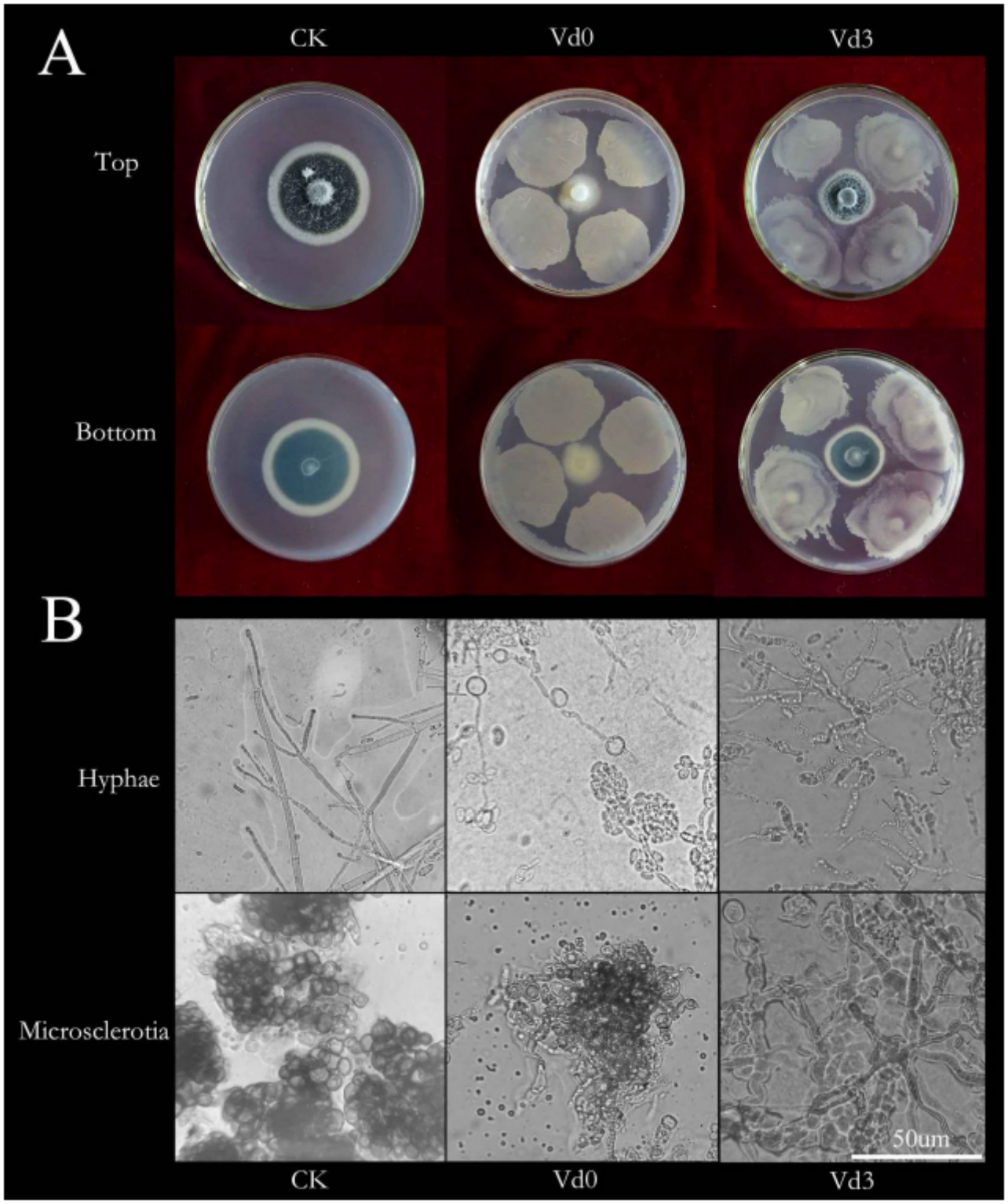

Figure 2

Observation of the phenotype of Verticillium dahliae. In vitro confrontation bioassays. (A) Pictures on the top and bottom show 9 cm PDA petri dishes of V. dahliae. Compared with the CK, the diameters of the community of Vd0 were significantly diminished, and the microsclerotia part of the Vd0 community is barely visible. (B) The hyphae and microsclerotia of V. dahliae under cedar oil at 1,000x magnification under an optical microscope. Microscopic examinations showed that the hyphae of the stress groups

were swollen, and the hyphae of Vd0 also showed rings and lysis. It is apparent that the microsclerotia of Vd0 are sparse and damaged.

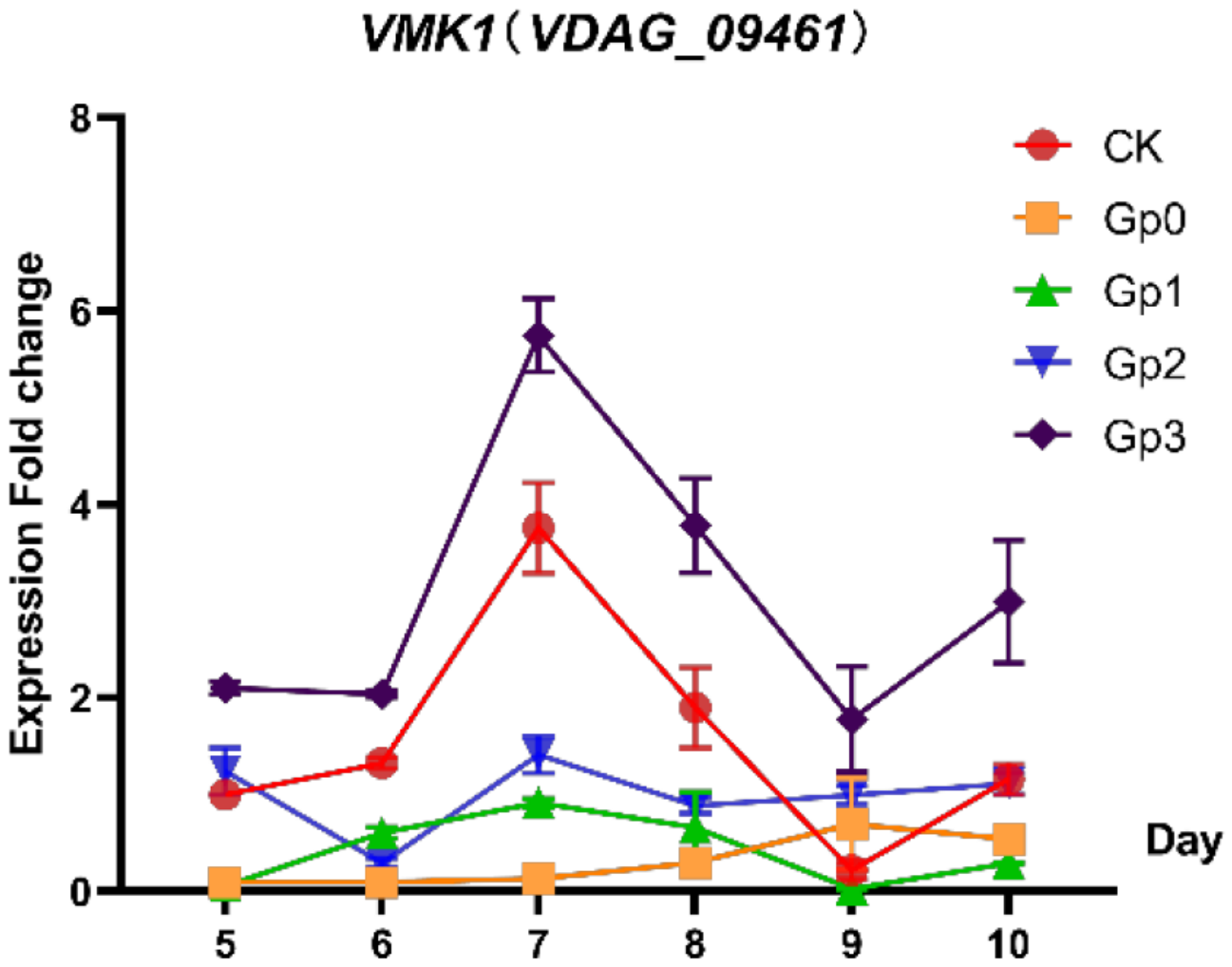

Figure 3

The expression of VMK1 gene in Verticillium dahliae in the CK, GP0, Gp1, GP2 and GP3 groups. In the CK, the X axis represents gene expression in V. dahliae cultured for 8 to 13 days and for the stress groups, the X axis represents gene expression in V. dahliae after interaction with Bacillus for 5 to 10 days.

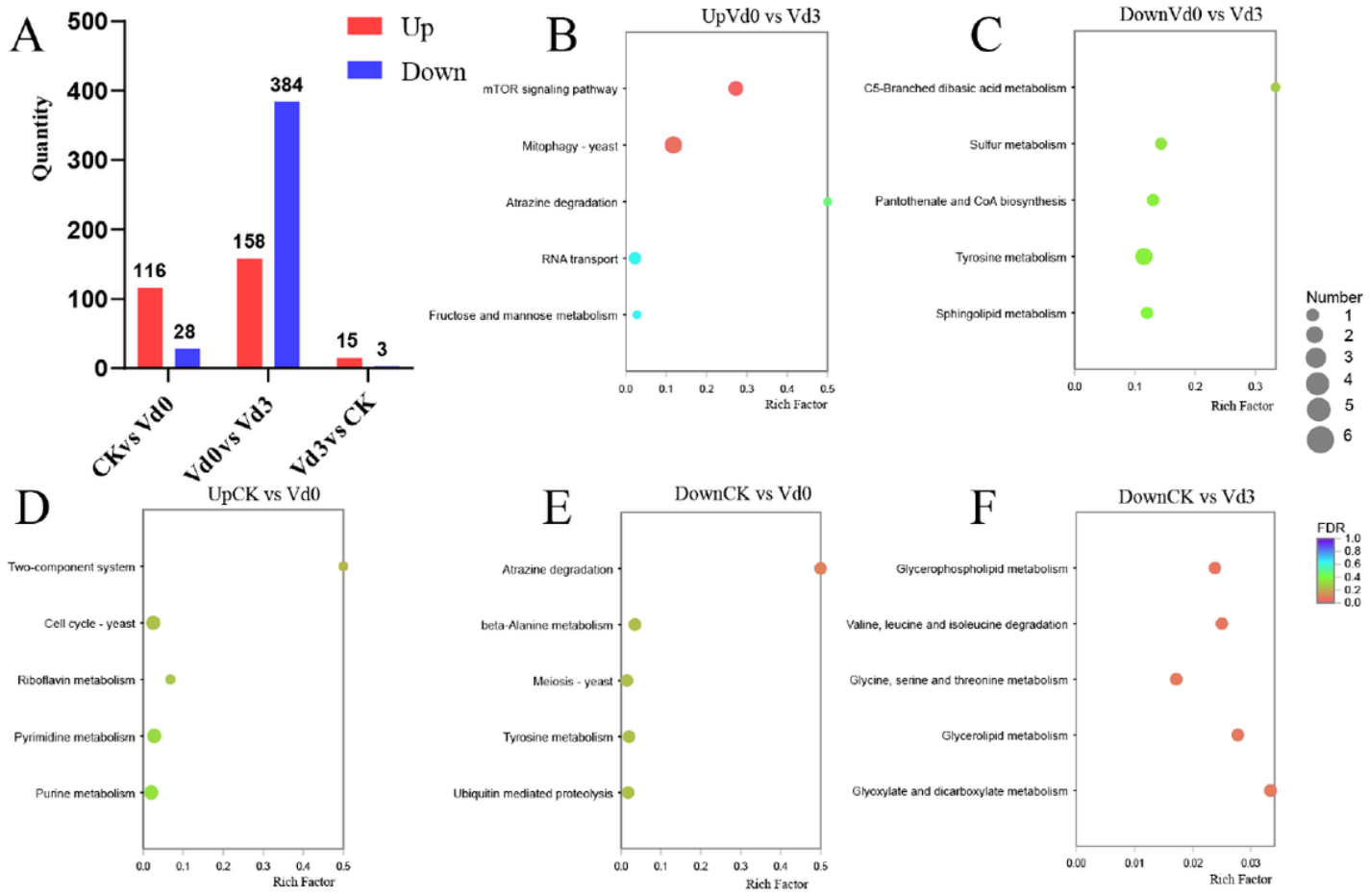

Figure 4

Statistics of the DEGs KEGG pathway enrichment. (A) DEGs were identified based on the criteria of P adjusted to < 0.05 and fold change ≥ 1.5 or ≤ 0.67. The Y axis on the right side represents the number of genes compared between the CK and Vd0, Vd0 and Vd3, Vd3 and CK. (B) Genes of the TOR and mitophagy pathways are significantly upregulated between Vd0 and Vd3($P < 0.05$). (C)-(F): There is no significant enrichment in the other DEGs. DEG, differentially expressed gene.

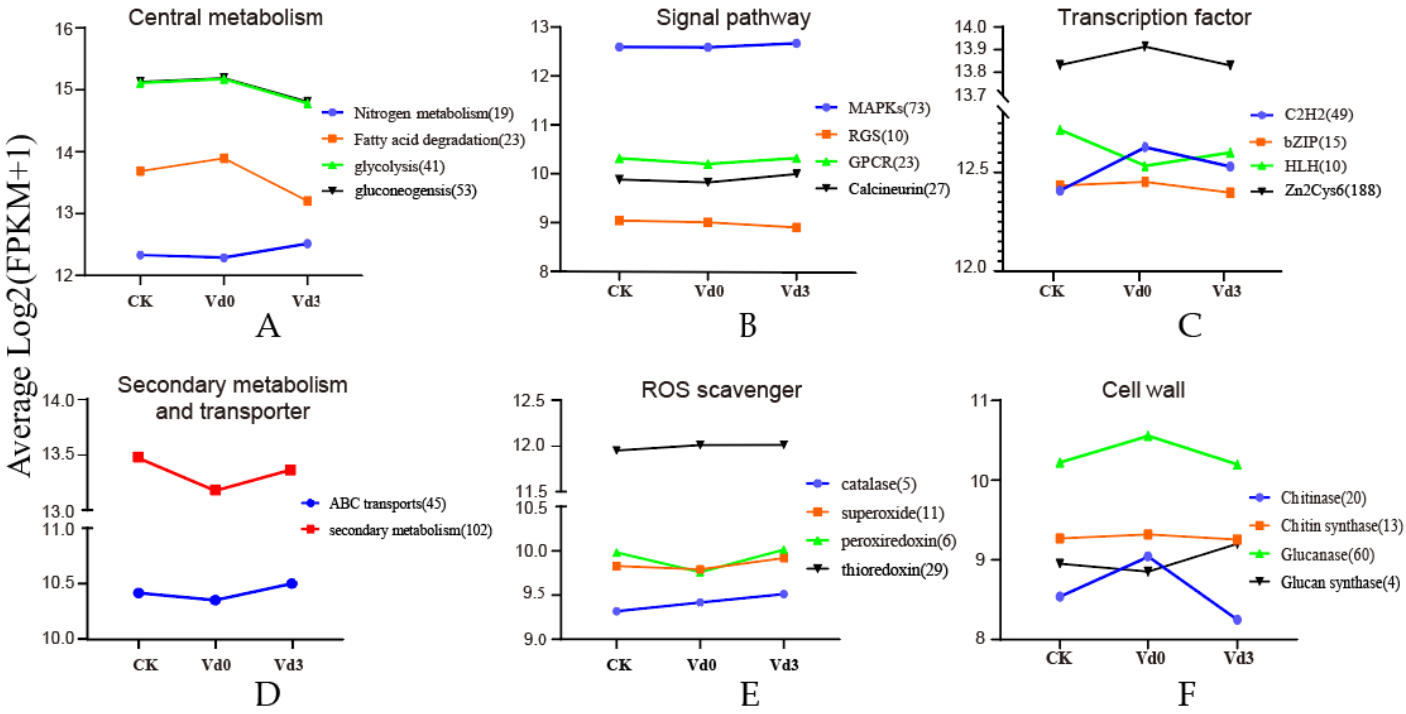

Figure 5

Patterns of expression of the genes in six functional categories. (A) The central metabolic pathways include nitrogen metabolism, fatty acid degradation, and glycolysis/gluconeogenesis. (B) Signal transduction and components, such as MAPK cascades, RGSs (regulators of G protein signaling), GPCR (G protein coupled receptors), and calcium signaling. (C) Four main classes of transcription factors, i.e., C2H2, bHLH, bZIP, and Zn2Cys6. (D) Secondary metabolism and ABC transporter genes. (E) ROS scavengers, i.e., catalase (CAT), superoxide dismutase (SOD), peroxiredoxin, and thioredoxin. (F) Enzymes related to the cell wall: chitinase, chitin synthase, glucanase, and glucan synthase, The Y axes are the log2-transformed total intensities. Total numbers within a gene family are shown in numerals, and the numbers of genes expressed within a family are shown in parentheses.

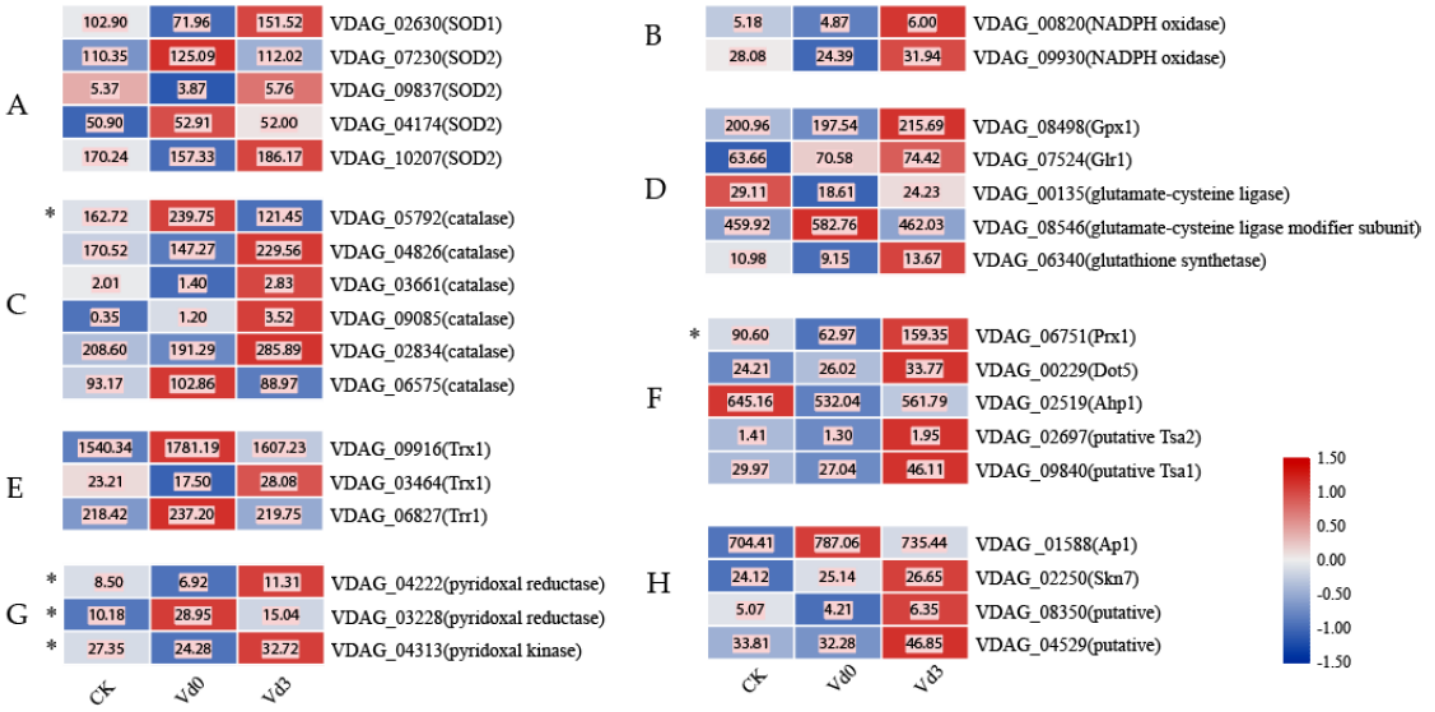

Figure 6

Profiles of the expression of genes from V. dahliae involved in ROS scavenging in the CK, Vd0, and Vd3 groups. The heatmap data was produced by TBtools and the symbol '*' represents significant regulation based on the criteria of P adjusted < 0.05 and fold change≥1.5 or ≤ 0.67 between Vd0 and Vd3. (A) Profiles of the expression of genes related to Cu- and Zn-superoxide dismutase (SOD). (B) Profiles of the expression of genes related to NADPH oxidase. (C) Profiles of the expression of genes related to catalase (CAT). (D) Profiles of the expression of genes related to the glutathione system. (E) Profiles of the expression of genes related to the peroxiredoxin system. (F) Profiles of the expression of genes related to transcription factors. (G) Profiles of the expression of genes related to pyridoxine. (H) Profiles of the expression of genes related to the thioredoxin system.

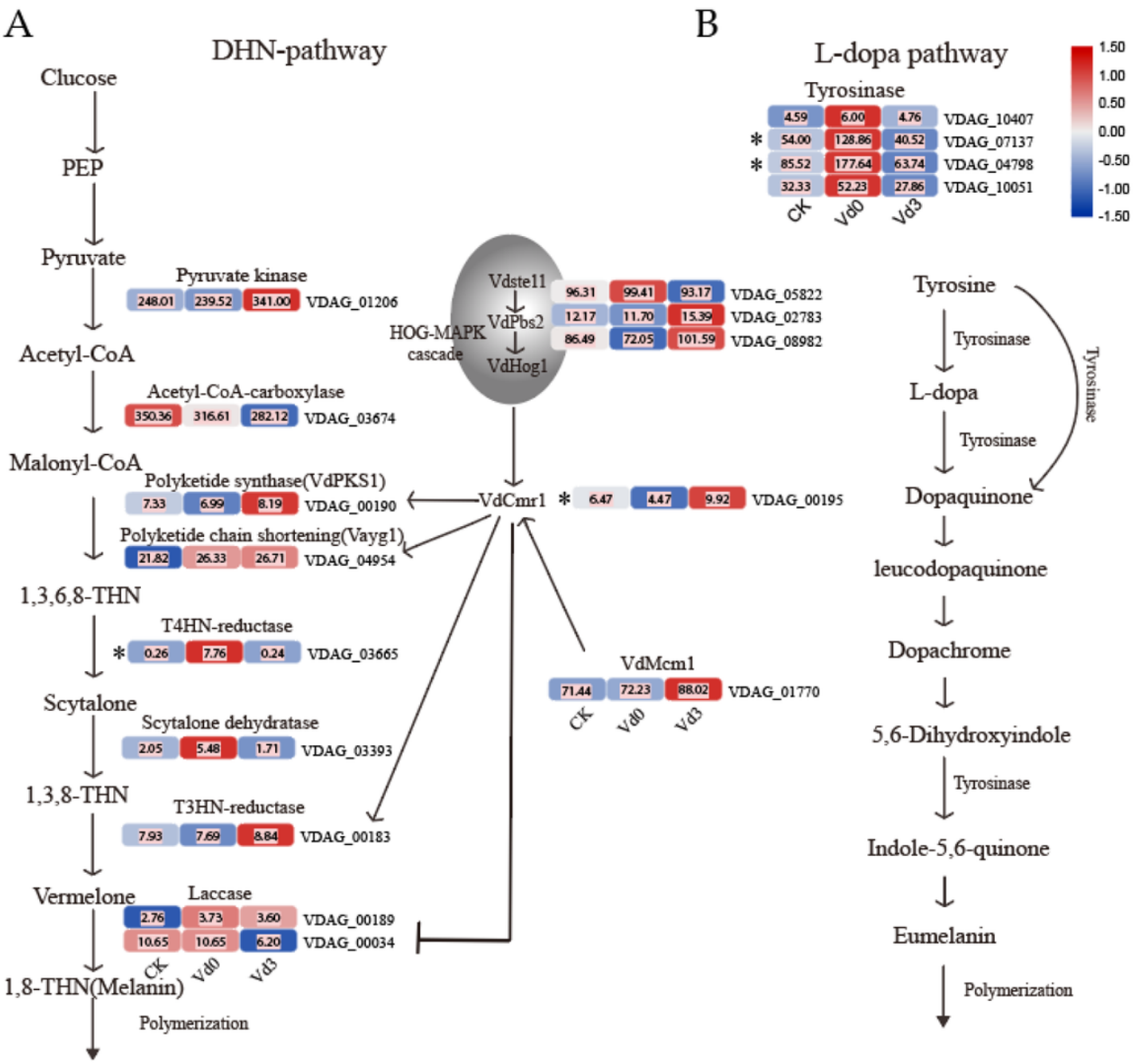

Figure 7

The profiles of expression and schematic diagram related to melanin production. The heatmap data was produced by TBtools and the symbol '*' represents significant regulation based on the criteria of P adjusted < 0.05 and fold change ≥1.5 or≤ 0.67 between Vd0 and Vd3. (A) DHN-pathway is referred by (Howlett et al. 2012). (B) The L-DOPA pathway is based on Tyrosine Metabolism in the KEGG Pathway.

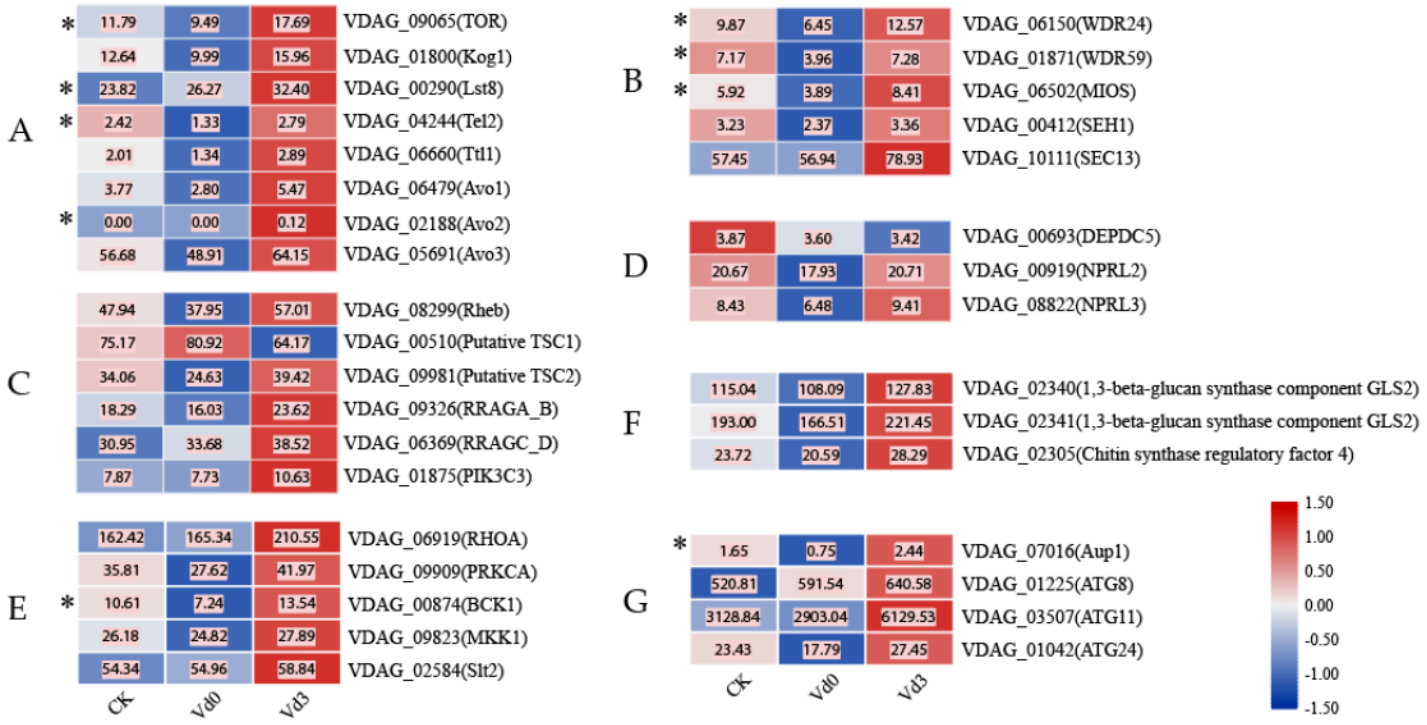

Figure 8

Profiles of the expression of genes from Verticillium dahliae related to glucan synthase, TOR, mitophagy, and CWI pathways in the CK, Vd0, and Vd3 groups. The heatmap data was produced by TBtools and the symbol '*' represents significant regulation based on the criteria of P adjusted <0.05 and fold change ≥1.5 or ≤ 0.67 between Vd0 and Vd3. (A) Profiles of the expression of genes related to components of the TOR complex. (B) Profiles of the expression of genes related to GATOR2. (C) Profiles of the expression of genes upstream of TORC. (D) Profiles of the expression of genes related to GATOR1. (E) Profiles of the expression of genes related to the CWI pathway. (F) Profiles of the expression of genes related to glucan synthase. (G) Profiles of the expression of genes related to mitophagy.

Supplementary Files

This is a list of supplementary files associated with this preprint. Click to download.

- Supplementarymaterial.pdf